Influence of excitability on unpinning and termination of spiral waves

Jiraporn Luengviriya,[1,2] Malee Sutthiopad,[3] Metinee Phantu,[3] Porramain Porjai,[3] Jarin Kanchanawarin,[3] Stefan C. Müller,[4] and Chaiya Luengviriya[3,*]

[1]*Department of Industrial Physics and Medical Instrumentation, King Mongkut's University of Technology North Bangkok, 1518 Pibulsongkram Road, Bangkok 10800, Thailand*

[2]*Lasers and Optics Research Group, King Mongkut's University of Technology North Bangkok, 1518 Pibulsongkram Road, Bangkok 10800, Thailand*

[3]*Department of Physics, Kasetsart University, 50 Phaholyothin Road, Jatujak, Bangkok 10900, Thailand*

[4]*Institute of Experimental Physics, Otto-von-Guericke University Magdeburg, Universitätsplatz 2, D-39106 Magdeburg, Germany*

(Received 16 June 2014; published 24 November 2014)

Application of electrical forcing to release pinned spiral waves from unexcitable obstacles and to terminate the rotation of free spiral waves at the boundary of excitable media has been investigated in thin layers of the Belousov-Zhabotinsky (BZ) reaction, prepared with different initial concentrations of H_2SO_4. Increasing $[H_2SO_4]$ raises the excitability of the reaction and reduces the core diameter of free spiral waves as well as the wave period. An electric current with density stronger than a critical value J_{unpin} causes a pinned spiral wave to drift away from the obstacle. For a given obstacle size, J_{unpin} increases with $[H_2SO_4]$. Under an applied electrical current, the rotation center of a free spiral wave drifts along a straight path to the boundary. When the current density is stronger than a critical value J_{term}, the spiral tip is forced to hit the boundary, where the spiral wave is terminated. Similar to J_{unpin} for releasing a pinned spiral wave, J_{term} also increases with $[H_2SO_4]$. These experimental findings were confirmed by numerical simulations using the Oregonator model, in which the excitability was adjusted via the ratio of the excitation rate to the recovery rate of the BZ reaction. Therefore, our investigation shows that decreasing the excitability can facilitate elimination of spiral waves by electrical forcing, either in the presence of obstacles or not.

DOI: 10.1103/PhysRevE.90.052919 PACS number(s): 05.45.−a, 05.65.+b, 82.40.Ck, 82.40.Qt

I. INTRODUCTION

Spiral waves have been observed in different reaction-diffusion systems including CO oxidation on platinum surfaces [1], concentration waves in the Belousov-Zhabotinsky (BZ) reaction [2], cell aggregation in slime mold colonies [3], and electrical wave propagation in cardiac tissues [4]. In the heart, such spiral waves of electrical excitation and their instabilities concern cardiac tachycardia and life-threatening fibrillations [5–7]. Drifting of electrophysiological spirals can cause the waves to end when their tip hits the boundary of the medium, but the tachycardia might last longer when the spiral waves are pinned to anatomical inhomogeneities or obstacles, e.g., veins or scars.

Theoretically, an inhomogeneity may induce the rotation center of spiral waves to orbit around it and the stability of the orbital path depends on the strength of the inhomogeneity [8]. In the vicinity of unexcitable obstacles, spiral waves move towards and are subsequently pinned to the obstacles [9,10]. Moreover, the wave period, wavelength, and velocity of pinned spiral waves increase with the obstacle size [11–13]. Scroll rings which are three-dimensional (3D) spiral structures with closed-loop filaments are often observed to contract and eventually self-annihilate [14,15]. Their intrinsic contraction is suppressed, when the scroll rings are pinned to obstacles [16,17].

Low-energy methods use a train of electrical stimuli with a sufficiently high frequency to induce unpinning and drift of spiral waves, until they collide with the boundary [18–21]. The necessary frequency increases with the obstacle size and the stimuli fail to release spiral waves being pinned to very large obstacles [18–21]. It has been demonstrated in numerical simulations [21] that reducing the excitability of a medium, resulting in an enlargement of the spiral core, can improve the success of unpinning induced by a train of stimuli. Similarly, prior experiments have shown that unpinning of spiral waves occurred after application of anti-arrhythmic agents, which reduced the excitability of cardiac specimens [22,23].

External application of an electric field can manipulate the dynamics of spiral waves in the BZ solutions, since it causes advective motions of ionic species in the reaction. In thin layers of this reaction, such a field forces the rotation center of free spiral waves to drift along a straight path, and the drift speed increases with the magnitude of the field [24–26]. In 3D media, the applied field causes the closed-loop filaments of free scroll rings to reorient, until the unit vector of the filaments is antiparallel to the field direction [15]. It has been demonstrated that such electric-field application causes reorientation and deformation of ring-shaped filaments that are pinned to a pair of unexcitable spheres, before the filaments are detached from these spheres [27]. Our recent investigation [28] on unpinning of spiral waves by electrical forcing revealed that it is more difficult to release spiral waves pinned to larger obstacles, especially when the obstacle size exceeds that of the core of free spiral waves.

In the absence of external forcing, the system boundary affects the motion of nearby spiral waves [29–32]. In BZ media, the spiral tip is found to drift along the boundary [29–31]; otherwise, it approaches and eventually hits the boundary [29,30] or moves away before the boundary effect becomes diminished [31]. Simulations [32] show that both

*Corresponding author: fscicyl@ku.ac.th

the center and the boundary of small media act as attractors of a spiral tip. Therefore, the spiral tip might be attracted to, induced to drift along, or repulsed away from the boundary, depending on its initial position.

It is worth noting that spiral waves, whose tip intrinsically drifts on a straight path in homogeneous media, may move until their tip hit and annihilate at the boundary [33]. However, this phenomenon might rarely occur in reality since the intrinsic drift has been observed in excitable media with very specific values of the parameters both in simulations [34] and in experiments [35]. In addition, spiral waves which drift either intrinsically [33] or are induced by a temporal modulation of excitability [36] are also discovered to reflect at the boundary so that they may always stay in the systems.

In this article, we present the influence of excitability on the release of pinned spiral waves and the termination of free spiral waves at the boundary by electrical forcing. The excitability of uniform thin layers of the BZ reaction was adjusted via initial concentration of sulfuric acid. Three series of experiments were undertaken to study (a) the intrinsic dynamics of free spiral waves (without obstacles), and electrically induced (b) release of spiral waves pinned to obstacles and (c) termination of free spiral waves at the boundary. Furthermore, we performed simulations using a reaction-diffusion-advection system with the Oregonator model [37,38] corresponding to all three experimental series.

II. EXPERIMENTS

A. Experimental methods

In this investigation, the BZ reaction is composed of $NaBrO_3$, malonic acid (MA), H_2SO_4, and ferroin, all purchased from Merck. In addition, a surfactant, sodium dodecyl sulfate (SDS, from Fluka), is added to the solution to reduce the production of CO_2 bubbles, which are uncontrollable inhomogeneities. Stock solutions of $NaBrO_3$ (1 M), and MA (1 M), and SDS (1 M) are freshly prepared by dissolving powder in deionized water (conductivity of $\sim 0.056\,\mu S\,cm^{-1}$), whereas stock solutions of H_2SO_4 (2.5 M) and ferroin (25 mM) are commercially available. Appropriate volumes of the stock solutions are mixed and diluted in deionized water to form BZ solutions with initial concentrations $[NaBrO_3] = 50$ mM, $[MA] = 50$ mM, $[\text{ferroin}] = 0.625$ mM, and $[SDS] = 0.05$ mM, where $[H_2SO_4]$ is varied between 100 and 280 mM. To prevent any hydrodynamic perturbation, the reaction is embedded in a 1.0% wt./wt. agarose gel (from Sigma).

In the first series of experiments, we study the influence of $[H_2SO_4]$ on the properties of free spiral waves in a uniform thin layer of the BZ reaction by measuring the wave period and the size of the spiral core—a circular area around which the spiral tip rotates. The tip position is defined as the intersection of contour lines of two subsequent spiral images at an interval of 5 s, which is very short as compared with the wave period of more than 2 min. Electrical forcing is utilized to release spiral waves pinned to inert plastic obstacles and to terminate free spiral waves at the boundary in the second and third series of experiments, respectively. The reactor has a main volume (size $100 \times 100 \times 1.0\,mm^3$) and its front plane (area $100 \times 100\,mm^2$) is set vertically oriented and normal to the camera viewing axis. Two electrolytic compartments (size of each is $25 \times 100 \times 2.0\,mm^3$) are attached to the left and the right boundaries of the main volume. An unexcitable obstacle (a plastic cylinder with a diameter d of 0.8 mm and a height of 1.0 mm) is attached in the main volume by using silicone paste, before the BZ solution is filled into the reactor.

Single spiral waves are initiated in the thin layers of the BZ reaction by a two-layer method as illustrated in [39] for free spiral waves and in [28] for pinned ones. In all experiments, the reactor is placed in a transparent thermostating bath to remove Ohmic heat and to set the temperature at 24 ± 1°C. The bath is put between a white light source and a color CCD camera (Super-HAD, Sony) to record the images of the medium every second with a resolution of $25 - 50\,\mu m\,pixel^{-1}$.

As a result of electrolysis, gas bubbles are produced near the electrodes and subsequently escape from the reactor. This causes temporal fluctuations of the resistance between the electrodes. To specify precisely the strength of forcing, electricity driven by a power supply in a constant electrical current mode is utilized. Therefore, the forcing is reported as electrical current density instead of electric field strength, which is usually used in simulations.

In the second series of experiments, the release of a pinned spiral wave by electrical forcing is investigated using the same strategy as in [28], which results in a precise critical value of electrical forcing while the aging of the BZ reaction can be minimized. For a given $[H_2SO_4]$, a constant current density J is applied to the medium for an interval of three to five spiral rotations, before it is increased by a step of $\Delta J = 10\,mA\,cm^{-2}$. When J is sufficiently high, the spiral tip is detached from the obstacle. This experiment gives a rough estimation of the critical current density for unpinning J_{rough}. Then, the experiment is repeated using a starting value J_0 close to but smaller than the rough estimation ($J_0 = J_{rough} - 10\,mA\,cm^{-2}$) and J is increased by $\Delta J = 2\,mA\,cm^{-2}$, which is the finest step available from our equipment. The latter experiment provides the minimal current density for unpinning, J_{unpin}, when the spiral wave is released from the obstacle.

Influence of excitability on forced termination of a free spiral wave at the boundary is studied in the third series of experiments, separate from the investigation of unpinning phenomena, for minimizing the aging of the BZ reaction. The free spiral wave is forced by an applied electrical current to approach the bottom of the reactor. When the electrical current is higher than a certain threshold, the spiral tip hits the boundary and the spiral wave is annihilated. As in the experiments of J_{unpin}, the minimal current density for termination J_{term} for a given $[H_2SO_4]$ is searched by two subsequent experiments with different steps $\Delta J = 10$ and $2\,mA\,cm^{-2}$, respectively.

It is worth noting that the container bottom is the most appropriate boundary for the study of spiral termination using our reactor, since the left and right edges of the main volume are in contact with electrolytic compartments and the top surface of the medium is opened to the atmosphere. The tip motion might be affected by undesired effects of electrolytic products (e.g., bubbles) and atmospheric oxygen, when the tip is in the vicinity of the lateral and the top edges, respectively.

B. Experimental results

In experiments of the intrinsic dynamics of free spiral waves, the excitability of the medium is modulated via the concentration of H_2SO_4. For $[H_2SO_4] = 100 - 280$ mM, the BZ reaction supports a rigidly rotating spiral wave, whose tip moves around a small circular region, the so-called spiral core. As shown in Fig. 1, both the wave period T and the spiral core diameter d_S of the free spiral wave decrease, when $[H_2SO_4]$ is increased.

The release of pinned spiral waves by electrical forcing is illustrated in Fig. 2. For all unpinning experiments we initiate a spiral wave whose tip is attached to the same unexcitable cylinder (diameter $d = 0.8$ mm) in a freshly prepared BZ medium. As an example, the pinned spiral wave in Fig. 2(a) is obtained from an experiment with $[H_2SO_4] = 200$ mM. Under an applied electrical current with a sufficiently strong density $J_{unpin} = 57\,mA\,cm^{-2}$, this pinned spiral wave is released, i.e., the tip is detached and drifts away from the obstacle, as shown in Fig. 2(b).

The results of unpinning at different $[H_2SO_4]$, as depicted in Fig. 2(c), reveal that it is necessary to apply an electrical current with a stronger density (higher J_{unpin}) to induce the unpinning phenomena, when the BZ reaction contains more H_2SO_4. Therefore, it is more difficult to release a spiral wave pinned to a given obstacle in a medium with higher excitability.

In Fig. 2(d) we consider the relation between J_{unpin} and the spiral core diameter d_S of a free spiral wave. This graph is obtained by matching J_{unpin} [from Fig. 2(c)] and d_S [from Fig. 1(b)] for each $[H_2SO_4]$. From the left to the right of this graph, d_S decreases from 1.20 mm to 0.45 mm, corresponding to an increase of $[H_2SO_4]$ from 100 mM to 280 mM, so that d_S ranges from a value larger to smaller than the obstacle diameter ($d = 0.8$ mm). The graph shows that J_{unpin} increases monotonously, while d_S decreases. Therefore, the smaller the free spiral core, the more difficult to unpin the spiral wave from a given obstacle.

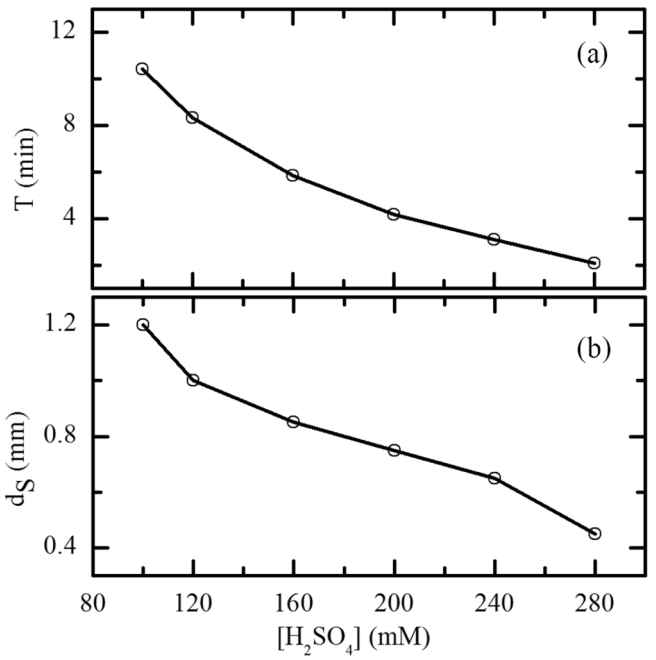

FIG. 1. Properties of a free spiral wave in the BZ reaction: (a) wave period T and (b) spiral core diameter d_S at different initial concentrations of H_2SO_4.

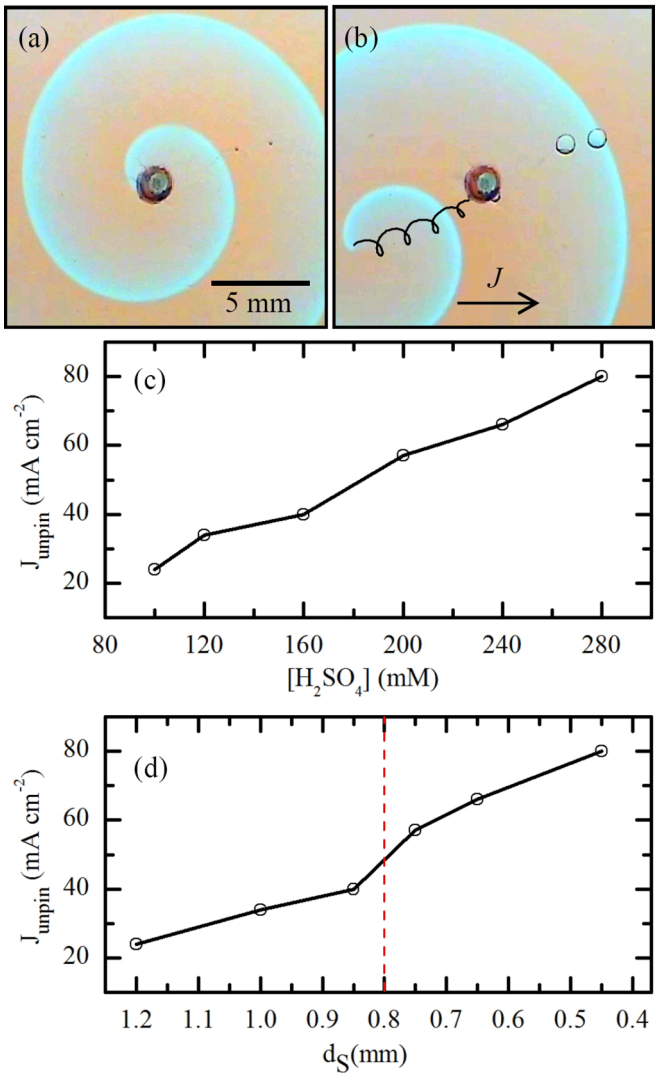

FIG. 2. (Color online) Unpinning of a spiral wave in the BZ reaction. (a) A spiral wave is pinned to a plastic cylinder. (b) When the density J of the applied electrical current reaches the critical value J_{unpin}, the spiral tip is unpinned. The black line indicates the tip trajectory of the released spiral wave moving away from the obstacle. (c) J_{unpin} vs $[H_2SO_4]$. (d) J_{unpin} vs core diameter d_S of a free spiral wave. The vertical dashed line at 0.8 mm indicates the diameter d of the obstacle.

Electrically forced termination of spiral waves at the boundary is shown in Fig. 3. At the beginning, an isolated spiral wave is initiated in the absence of obstacles. The spiral tip is located around 1 cm away from the bottom of the reactor [blue (bright) front in Fig. 3(a)]. At this distance, the spiral tip rotates on a circular path implying that it is not affected by the boundary. A constant electrical current induces the tip to drift along a tilted direction towards the bottom [see the red (gray) line]. Note that the spiral tip drifts almost antiparallel to the current direction when it is located near

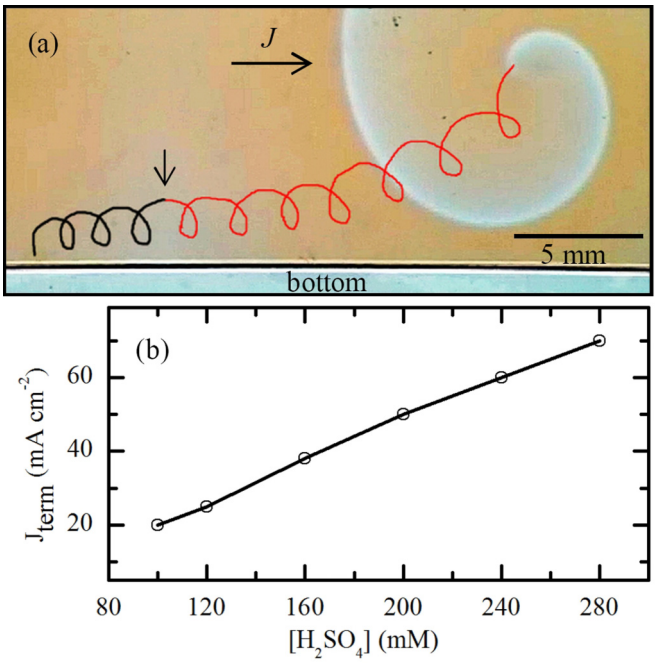

FIG. 3. (Color online) Termination of a free spiral wave in the BZ reaction. (a) An applied electrical current with density J induces a drift of the spiral tip towards the bottom of the reactor [red (gray) line]. When the tip is located near the boundary, it drifts approximately antiparallel to the current direction. After J is increased to a critical value (J_{term}), the tip (location indicated by the vertical arrow) gradually approaches and finally hits the bottom (black line). (b) J_{term} increases with [H_2SO_4].

the bottom. The magnitude of electrical current density is increased, until the spiral tip is forced to hit the bottom and subsequently annihilated (see the black line). Figure 3(a) is obtained from an experiment at [H_2SO_4] = 100 mM, where the necessary current density of spiral termination $J_{term} = 20\,\text{mA cm}^{-2}$. Figure 3(b) depicts the results from a series of termination experiments with different [H_2SO_4]. Similar to J_{unpin} in Fig. 2(c), J_{term} increases with [H_2SO_4]. Therefore, it is more difficult to terminate a spiral wave at the boundary of a medium that has a higher excitability.

III. SIMULATIONS

A. Simulation methods

To corroborate the experimental results, simulations are performed using the two-variable Oregonator model to describe the dynamics of two variables u and v (corresponding to the concentrations of $HBrO_2$ and the catalyst, respectively) in the BZ reaction. The advection terms for both u and v account for the electric field E applied in the x direction:

$$\frac{\partial u}{\partial t} = \frac{1}{\varepsilon}\left(u - u^2 - fv\frac{u-q}{u+q}\right) + D_u\nabla^2 u - M_u E\frac{\partial u}{\partial x},$$
$$\frac{\partial v}{\partial t} = u - v + D_v\nabla^2 v - M_v E\frac{\partial v}{\partial x}. \quad (1)$$

To obtain rigidly rotating spiral waves in the absence of the electric field, the parameters are chosen as in Ref. [38]: $q = 0.002$, $f = 1.4$, diffusion coefficients $D_u = 1.0$ and $D_v = 0.6$, with the excitability modulated by parameter $\varepsilon^{-1} = 20 - 200$. As in [15,28], when the electric field is applied, the ionic mobilities M_u and M_v are set to -1.0 and 2.0, respectively. The simulations are performed using an explicit Euler method with a nine-point approximation of the two-dimensional Laplacian operator and a centered-space approximation of the gradient term.

The influence of excitability on the intrinsic dynamics of a free spiral wave as well as spiral termination at a boundary induced by an electric field are studied on a discrete system with a uniform grid space $\Delta x = \Delta y = 0.1$ system unit (s.u.) and a time step $\Delta t = 3.0 \times 10^{-3}$ time unit (t.u.), as required for numerical stability [$\Delta t \leqslant (3/8)(\Delta x)^2$ [40]]. The dimensionless size of the system is 40×40 s.u. (corresponding to 400×400 grid points) and the boundaries of the system have no-flux conditions. A spiral wave is initiated as follows: a planar wave is triggered by setting a five-grid-point strip at an edge of the medium to an excited state (e.g., $u = 1.0$ and $v = 0$ for $0.0 \leqslant x \leqslant 0.5$). When the wave front propagates into the middle of the medium, half of the medium is reset to an excitable state (e.g., $u = 0$ and $v = 0$ for $0.0 \leqslant y \leqslant 20.0$) leading to a free-end wave front, which subsequently curls to form a rotating spiral wave. As in the experimental part, the spiral tip is defined as the intersection of contour lines of two subsequent (delaytime $= 1.5 \times 10^{-2}$ t.u.) spiral images (u fields). In the simulations of spiral termination by electric field, the spiral tip is induced to drift towards and hit the bottom of the system.

The release of a pinned spiral wave by an electric field at different excitability is investigated on a finer discrete system, in order to construct a good approximation of an unexcitable circular obstacle. As in Ref. [28], we set the uniform grid space $\Delta x = \Delta y = 0.025$ s.u. and the time step $\Delta t = 1.9 \times 10^{-4}$ t.u., while the size of the system is reduced to 20×20 s.u. (corresponding to 800×800 grid points). After the spiral wave is allowed to propagate freely for several rotations, a circular obstacle, i.e., a group of discrete points (x, y) in which $\sqrt{(x-x_0)^2 + (y-y_0)^2} \leqslant d/2$, where diameter $d = 1.0$ s.u., is placed at the spiral core center (x_0, y_0). In contrast to the phase-field methods used in [27,41,42], we explicitly determine the boundary between the obstacle and the medium as a group of points (P) (located outside but adjacent to the obstacle) which forms a closed-loop boundary wrapping around the unexcitable obstacle and has no-flux conditions. To calculate the 2D diffusion terms [in Eq. (1)] at each point P, one needs u and v at P and its eight neighboring points in 3×3 matrices. For those neighboring points located in the obstacle, their u and v are copied from the opposite elements in the matrices. The same method is applied for the gradient terms [in Eq. (1)] with 1×3 matrices.

B. Simulation results

Our simulation system [Eq. (1)] supports rigidly rotating spiral waves with intrinsic dynamics depending on the parameter ε^{-1}. When ε^{-1} is increased, the excitability becomes stronger, but both the wave period T and the spiral core diameter d_S of the free spiral waves decrease, as shown in Fig. 4.

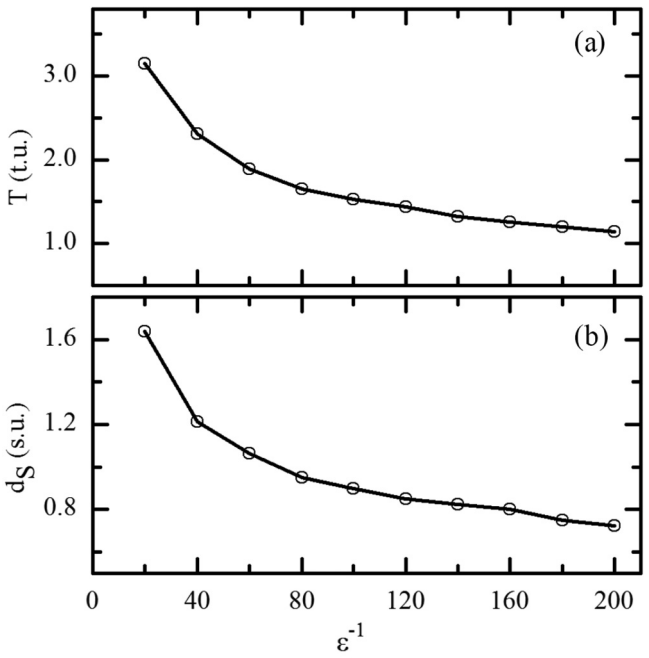

FIG. 4. Properties of free spiral waves in the Oregonator model: (a) wave period and (b) diameter of spiral core at different excitability (ε^{-1}). t.u. and s.u. stand for time and system units, respectively.

The influence of the excitability on the release of pinned spiral waves by an electrical field is depicted in Fig. 5. For instance, Figs. 5(a)–5(f) demonstrates an unpinning of a spiral wave from an unexcitable circular obstacle (diameter $d = 1.0$ s.u.) in a simulation with $\varepsilon^{-1} = 100$. In this case, the sufficiently strong electric field E_{unpin} is 0.335. For a short interval in the beginning, the spiral wave is still attached to the obstacle until its tip is located at the left of the obstacle [Fig. 5(a)]. Then, the spiral tip is detached and moves away from the obstacle for a short distance [Fig. 5(b)], before it bounces back and touches the obstacle again [Fig. 5(c)]. Subsequently, the spiral wave is detached for the second time [Fig. 5(d)] and gradually drifts away from the obstacle in the course of time [Figs. 5(e) and 5(f)]. Such forced temporary detachment as in Figs. 5(a)–5(c) is not observed in our experiments. As discussed in our earlier report [28], the finest step of the electrical current density ($\Delta J = 2\,\text{mA cm}^{-2}$) might be insufficiently small to allow it to occur.

Simulations of the release of a spiral wave at different ε^{-1} are summarized in Fig. 5(g). For a given obstacle, the necessary electric field E_{unpin} increases monotonously with ε^{-1}. This means that it is more difficult to release a pinned spiral wave in the Oregonator model at higher excitability (higher ε^{-1}). Figure 5(h) depicts a plot of E_{unpin} and the core diameter d_S of a free spiral wave. It is derived by matching E_{unpin} [from Fig. 5(g)] and d_S [from Fig. 4(b)] for each ε^{-1}. To the right of the graph, d_S is reduced from larger to smaller size as compared to the obstacle diameter ($d = 1.0$ s.u.). This graph shows that E_{unpin} increases when d_S decreases and qualitatively agrees with that from the experiments in Fig. 2(d).

The termination of spiral waves at the boundary induced by an electric field is shown in Fig. 6. To mimic the experiments, an isolated spiral wave is initiated at the lower-right part of

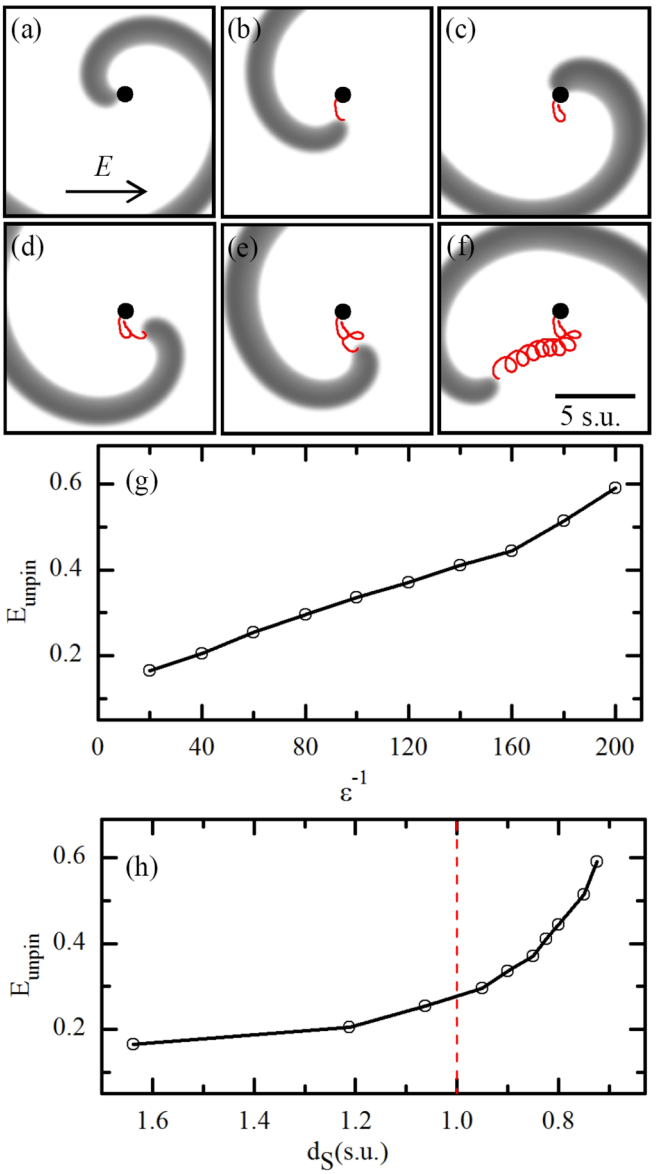

FIG. 5. (Color online) Unpinning of a spiral wave in the Oregonator model. Sequential images (a)–(f) illustrate an unpinning phenomenon induced by the critical electric field E_{unpin} at $t = 0.77$, 1.32, 2.07, 3.40, 4.77, and 15.88 t.u., respectively. Red (gray) lines in (b)–(f) indicate the trajectory of the spiral tip. See the text for detail. (g) E_{unpin} vs the parameter ε^{-1}. (h) E_{unpin} vs the core diameter d_S of a free spiral wave. The vertical dashed line at 1.0 s.u. indicates the diameter d of the obstacle.

the system. Figure 6(a) demonstrates an example of a spiral termination for $e^{-1} = 100$. The spiral tip is initially located about 5 and 10 s.u. away from the right and bottom edges, respectively. The spiral tip moves on a small circle since there is no boundary effect on the tip. Under an electric field $E = 0.370$, this spiral tip drifts along a tilted direction towards the bottom before it moves almost antiparallel to the field direction [see the red (gray) line]. Then the spiral tip is forced to hit the bottom by a tiny stronger field $E_{\text{term}} = 0.375$, so that the spiral wave is terminated (see the black line). Figure 3(b) summarizes the results from the simulations

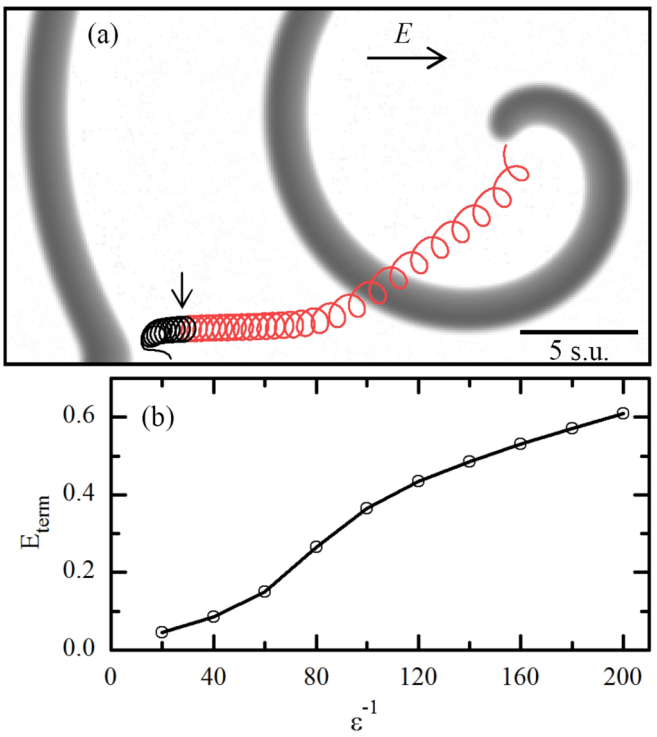

FIG. 6. (Color online) Termination of a free spiral wave in the Oregonator model. (a) An applied electric field E induces a drift of the spiral tip towards the bottom of the system [red (gray) line]. When the tip is located near the boundary, it drifts approximately antiparallel to the direction of E. After E is increased to a critical value (E_{term}), the tip (location indicated by the vertical arrow) gradually approaches and finally hits the boundary (black line). (b) E_{term} increases with parameter ε^{-1}.

of spiral termination for different ε^{-1}. The critical electric field E_{term} increases with ε^{-1}. Therefore, the stronger the excitability, the more difficult it becomes to terminate a spiral wave at the boundary.

IV. DISCUSSION AND CONCLUSION

We have presented an investigation of the release of a pinned spiral wave and the termination of a free spiral wave at the system boundary by electrical forcing at different excitabilities. The results from experiments using the BZ reaction (Figs. 1–3) were qualitatively reproduced in simulations using the Oregonator model (Figs. 4–6). The excitabilities of the BZ reaction and the Oregonator model increase with $[H_2SO_4]$ and the parameter ε^{-1}, respectively. While the excitability rises, both the period and the core diameter of a free spiral wave decrease (see Figs. 1 and 4).

For a given obstacle, the necessary value of electrical forcing for releasing a pinned spiral wave grows with the excitability [Figs. 2(c) and 5(g)]. These findings agree well with earlier numerical simulations [21] and cardiac experiments [22,23] which show that reducing excitability can facilitate the unpinning of a spiral wave. In addition, the electrically forced unpinning concerns both the size of the free spiral core and that of the obstacle as follows. The required magnitude of electrical forcing increases if the free spiral core becomes smaller [Figs. 2(d) and 5(h)]. Our recent report [28] shows that the electrical forcing increases with the obstacle diameter while the spiral core diameter is fixed. Therefore, either an enlargement of the free spiral core or a reduction of the obstacle size results in the required strength of forcing to decrease.

The boundary effect on a spiral wave is comparable to the interaction of a symmetrical counter-rotating spiral pair, i.e., the single spiral wave interacts with its mirror while the boundary is acting as the axis of symmetry of the spiral pair [31]. Here, we qualitatively compare our results of the spiral termination at boundary [Figs. 3(a) and 6(a)] to the dynamics of a spiral pair under electrical forcing reported in [43,44]. In Figs. 3(a) and 6(a), an electrical forcing induces the spiral tip (far from the boundary) to drift with an angle to the applied field at the beginning. While the tip moves towards the boundary, the drift direction gradually changes until parallel to the boundary. We conjecture that the component of the drift velocity perpendicular to the boundary decreases until it vanishes due to the repulsion of the boundary. These results are very similar to the forcing of a spiral pair in [43] in which the tilted trajectories of both drifting spiral tips become parallel to the axis of symmetry. For sufficient strong forcing, the spiral tip approaches and hits the boundary at final state in Figs. 3(a) and 6(a). We conjecture that the repulsion of the boundary is overcome by the strong forcing or the tip moves into "the attractive zone" of the boundary as in [29–32]. This forced termination is comparable to the forced annihilation of a spiral pair in [44]. Furthermore, our results also show that the critical value of electrical forcing for terminating a free spiral wave at the boundary also increases with the excitability [Figs. 3(b) and 6(b)].

In summary, our findings in both parts of the spiral unpinning and the spiral termination at boundary induced by electrical forcing imply that weakening of the excitability of the medium helps to eliminate spiral waves both with and without obstacles. This contribution together with earlier reports [21–23] demonstrates that the excitability plays an important role in successfully eliminating spiral waves, in general, for different methods of elimination as well as different excitable media.

ACKNOWLEDGMENTS

We thank the Faculty of Science, the Research and Development Institute (KURDI), the Center for Advanced Studies of Industrial Technology, and the Graduate School, Kasetsart University, the German Academic Exchange Service (DAAD), and the Office of the Higher Education Commission and King Mongkut's University of Technology North Bangkok (Contract No. KMUTNB-NRU-57-11) for financial support.

[1] S. Nettesheim, A. von Oertzen, H. H. Rotermund, and G. Ertl, J. Chem. Phys. **98**, 9977 (1993).
[2] A. T. Winfree, Science **175**, 634 (1972).
[3] F. Siegert and C. Weijer, J. Cell Sci. **93**, 325 (1989).

[4] J. M. Davidenko, A. M. Pertsov, R. Salomonz, W. Baxter, and J. Jalife, Nature (London) **355**, 349 (1992).
[5] A. T. Winfree, Science **266**, 1003 (1994).
[6] R. A. Gray, A. M. Pertsov, and J. Jalife, Nature (London) **392**, 75 (1998).
[7] F. Fenton, E. M. Cherry, H. M. Hastings, and S. J. Evans, Chaos **12**, 852 (2002).
[8] V. N. Biktashev, D. Barkley, and I. V. Biktasheva, Phys. Rev. Lett. **104**, 058302 (2010).
[9] A. P. Muñuzuri, V. Pérez-Muñuzuri, and V. Pérez-Villar, Phys. Rev. E **58**, R2689 (1998).
[10] C. W. Zemlin and A. M. Pertsov, Phys. Rev. Lett. **109**, 038303 (2012).
[11] J. P. Keener and J. J. Tyson, Physica D **21**, 307 (1986).
[12] Y.-Q. Fu, H. Zhang, Z. Cao, B. Zheng, and G. Hu, Phys. Rev. E **72**, 046206 (2005).
[13] O. Steinbock and S. C. Müller, Physica A **188**, 61 (1992).
[14] K. I. Agladze, R. A. Kocharyan, and V. I. Krinsky, Physica D **49**, 1 (1991).
[15] C. Luengviriya, S. C. Müller, and M. J. B. Hauser, Phys. Rev. E **77**, 015201 (2008).
[16] Z. Jiménez, B. Marts, and O. Steinbock, Phys. Rev. Lett. **102**, 244101 (2009).
[17] Z. Jiménez and O. Steinbock, Europhys. Lett. **91**, 50002 (2010).
[18] K. Agladze, M. W. Kay, V. Krinsky, and N. Sarvazyan, Am. J. Physiol. Heart Circ. Physiol. **293**, H503 (2007).
[19] A. Isomura, M. Hörning, K. Agladze, and K. Yoshikawa, Phys. Rev. E **78**, 066216 (2008).
[20] M. Tanaka, A. Isomura, M. Hörning, H. Kitahata, K. Agladze, and K.Yoshikawa, Chaos **19**, 043114 (2009).
[21] A. Pumir, S. Sinha, S. Sridhar, M. Argentina, M. Hörning, S. Filippi, C. Cherubini, S. Luther, and V. Krinsky, Phys. Rev. E **81**, 010901(R) (2010).
[22] Z. Y. Lim, B. Maskara, F. Aguel, R. Emokpae, and L. Tung, Circulation **114**, 2113 (2006).
[23] C. Cabo, A. M. Pertsov, J. M. Davidenko, W. T. Baxter, R. A. Gray, and J. Jalife, Biophys. J. **70**, 1105 (1996).
[24] O. Steinbock, J. Schütze, and S. C. Müller, Phys. Rev. Lett. **68**, 248 (1992).
[25] K. I. Agladze and P. De Kepper, J. Phys. Chem. **96**, 5239 (1992).
[26] A. P. Muñuzuri, V. A. Davydov, V. Pérez-Muñuzuri, M. Gómez-Gesteira, and V. Pérez-Villar, Chaos Solitons Fractals **7**, 585 (1996).
[27] Z. A. Jiménez, Z. Zhang, and O. Steinbock, Phys. Rev. E **88**, 052918 (2013).
[28] M. Sutthiopad, J. Luengviriya, P. Porjai, B. Tomapatanaget, S. C. Müller, and C. Luengviriya, Phys. Rev. E **89**, 052902 (2014).
[29] V. S. Zykov and S. C. Müller, Physica D **97**, 322 (1996).
[30] M. Gómez-Gesteira, A. P. Muñuzuri, V. Pérez-Muñuzuri, and V. Pérez-Villar, Phys. Rev. E **53**, 5480 (1996).
[31] H. Brandtstädter, M. Braune, I. Schebesch, and H. Engel, Chem. Phys. Lett. **323**, 145 (2000).
[32] J. Yang and M. Zhang, Phys. Lett. A **352**, 69 (2006).
[33] D. Olmos, Phys. Rev. E **81**, 041924 (2010).
[34] D. Barkley, Phys. Rev. Lett. **72**, 164 (1994).
[35] G. Li, Q. Ouyang, V. Petrov, and H. L. Swinney, Phys. Rev. Lett. **77**, 2105 (1996).
[36] J. Langham and D. Barkley, Chaos **23**, 013134 (2013).
[37] R. J. Field and R. M. Noyes, J. Chem. Phys. **60**, 1877 (1974).
[38] W. Jahnke and A. T. Winfree, Int. J. Bifurcat. Chaos **1**, 445 (1991).
[39] C. Luengviriya, U. Storb, M. J. B. Hauser, and S. C. Müller, Phys. Chem. Chem. Phys. **8**, 1425 (2006).
[40] M. Dowle, R. M. Mantel, and D. Barkley, Int. J. Bifurcat. Chaos **7**, 2529 (1997).
[41] F. H. Fenton, E. M. Cherry, A. Karma, and W.-J. Rappel, Chaos **15**, 013502 (2005).
[42] J. Kockelkoren, H. Levine, and W.-J. Rappel, Phys. Rev. E **68**, 037702 (2003).
[43] B. Schmidt and S. C. Müller, Phys. Rev. E **55**, 4390 (1997).
[44] J. Schütze, O. Steinbock, and S. C. Müller, Nature (London) **356**, 45 (1992).